ACSNANO
www.acsnano.org
ARTICLE

Kirigami Nanocomposites as Wide-Angle Diffraction Gratings

Lizhi Xu,[†,‡] Xinzhi Wang,[†,§] Yoonseob Kim,[†] Terry C. Shyu,[‡] Jing Lyu,[†,⊥] and Nicholas A. Kotov*[,†,‡,∥,¶]

[†]Department of Chemical Engineering, [‡]Department of Materials Science and Engineering, and [∥]Biointerfaces Institute, University of Michigan, Ann Arbor, Michigan 48109, United States

[§]School of Energy Science and Engineering, Harbin Institute of Technology, Harbin, Heilongjiang 150001, People's Republic of China

[⊥]School of Materials Science and Engineering, Northwestern Polytechnical University, Xi'an, Shaanxi 710072, People's Republic of China

[¶]Michigan Center for Integrative Research in Critical Care, Ann Arbor, Michigan 48109, United States

Supporting Information

ABSTRACT: **Beam steering devices represent an essential part of an advanced optics toolbox and are needed in a spectrum of technologies ranging from astronomy and agriculture to biosensing and networked vehicles. Diffraction gratings with strain-tunable periodicity simplify beam steering and can serve as a foundation for light/laser radar (LIDAR/LADAR) components of robotic systems. However, the mechanical properties of traditional materials severely limit the beam steering angle and cycle life. The large strain applied to gratings can severely impair the device performance both in respect of longevity and diffraction pattern fidelity. Here, we show that this problem can be resolved using micromanufactured kirigami patterns from thin film nanocomposites based on high-performance stiff plastics, metals, and carbon nanotubes, *etc.* The kirigami pattern of microscale slits reduces the stochastic concentration of strain in stiff nanocomposites including those made by layer-by-layer assembly (LBL). The slit patterning affords reduction of strain by 2 orders of magnitude for stretching deformation and consequently enables reconfigurable optical gratings with over a 100% range of period tunability. Elasticity of the stiff nanocomposites and plastics makes possible cyclic reconfigurability of the grating with variable time constant that can also be referred to as 4D kirigami. High-contrast, sophisticated diffraction patterns with as high as fifth diffraction order can be obtained. The angular range of beam steering can be as large as 6.5° for a 635 nm laser beam compared to ∼1° in surface-grooved elastomer gratings and ∼0.02° in MEMS gratings. The versatility of the kirigami patterns, the diversity of the available nanocomposite materials, and their advantageous mechanical properties of the foundational materials open the path for engineering of reconfigurable optical elements in LIDARs essential for autonomous vehicles and other optical devices with spectral range determined by the kirigami periodicity.**

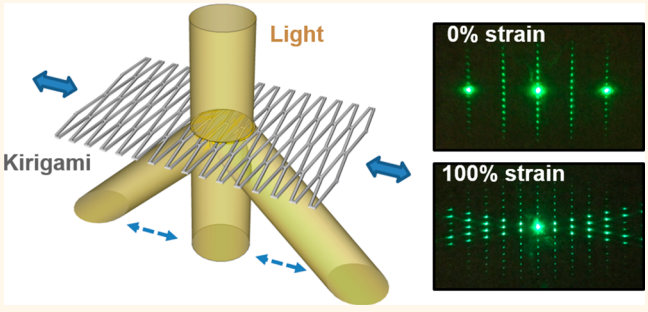

KEYWORDS: *kirigami materials, 4D kirigami, nanocomposites, adaptive optics, layer-by-layer assembly, stretchable devices, LIDARS, LADARs, autonomous vehicles, robots, perception systems*

Dynamic steering of optical beams is central for information technologies, optical data storage, biomedical diagnostics, precision agriculture, weather predictions, autonomous vehicles, and other future and current technologies. For instance, beam steering optical elements are central to light/laser radars (LIDARs or LADARs) and typically are being implemented with a set of actuated mirrors. More recent beam steering devices based on spatial light modulation, such as optical phased arrays,[1] electro-optic and acousto-optic modulators utilizing advanced optical materials, such as liquid crystals, ceramics, and photonic crystals, provide powerful and versatile methods of optical modulation including beam steering. However, they are also associated with pixel size limits, limited dynamic range, cross-talk of optical elements, and high cost, restricting their implementations.[2−7] Size and weight requirements can also be essential for LIDARs and other devices for airborne and other vehicles as well as as personal perception systems (PEPERS).

Received: March 26, 2016
Accepted: May 6, 2016
Published: May 6, 2016

DOI: 10.1021/acsnano.6b02096
ACS Nano 2016, 10, 6156−6162

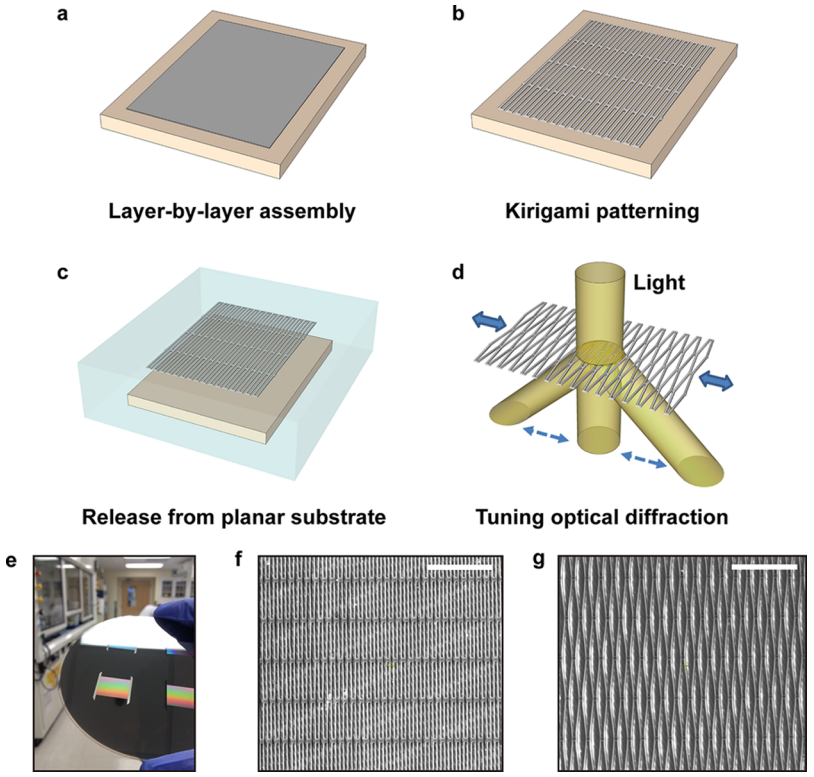

Figure 1. Nanocomposite kirigami as strain-tunable optical gratings. (a–d) Schematic illustration of the key steps in device processing. (e) Optical image of NKGs fabricated on a wafer. (f,g) SEM images of a NKG based on Cr/Parylene C nanocomposites under 0% (f) and 100% (g) strain. Scale bars: 50 μm.

Diffraction gratings with tunable periodicity represent promising alternatives for dynamic modulation of beam directionality due to light weight, low cost, and operational simplicity. However, realization of time-modulated diffraction gratings remains a challenge due to the limited strain tolerance of conventional materials. For example, performance of stretchable gratings based on silicone elastomers with surface microgrooves and coatings is impaired at high strains.[8−12] Cracking of metal coatings and/or stochastic, inhomogeneous strain distribution under large deformation are the major concerns for strain-tunable gratings based on elastomers.[8,11] Consequently, these gratings can rarely function at elongations beyond 30%, which is far below the deformation limit of constituent elastomers. Narrow temperature range for such gratings associated with the glass temperature transition of polymers represents another concern. Moreover, high Poisson's ratio of typical elastomers results in undesirable correlated expansion-contraction along presumably independent axes which scrambles the diffraction patterns at high strains.

Gratings utilizing micro-electro-mechanical systems (MEMS) represent another platform for beam steering and optical modulation. However, the characteristic scale of typical MEMS gratings is much longer than optical wavelengths.[13] Small dynamic range of angles, complex manufacturing process, rapid fatigue of ceramic components, and high cost can be a concern for many technologies exemplified by autonomous vehicles, agriculture, and PEPERS.[13,14]

The core issue of tunable diffraction gratings is, in fact, a *materials* engineering challenge. The principal material of the grating must meet difficult benchmarks with respect to optics, mechanics, and chemistry. While optical requirements for tunable gratings have been investigated by multiple groups,[8−11,14] the last two sets of properties and opportunities for the large library of nanomaterials are still to be addressed. Chemistry of nanomaterials affords fabrication techniques that can improve both the contrast and the dynamic range while simplifying the patterning process. Furthermore, materials for durable tunable gratings must possess high toughness, stiffness, and strength in order to retain microscale periodicity under large, cyclic deformations. Combining some of these properties, such as high stiffness and high strain, is a long-standing materials problem. The manifestation of this fundamental dilemma of material mechanics can be seen in the fact that reconfigurable diffraction gratings from high strength plastics have not been possible so far because they do not possess the ability to sustain high strains. Multiscale engineering of nanocomposites could enable significant improvements in materials mechanics and therefore functionality and practicality of reconfigurable diffraction gratings.

Recently, strain engineering through introduction of patterned cuts in thin film materials—an approach inspired by kirigami arts—attracted extensive academic attention.[15−25] Notches in kirigami sheets and folds in origami structures can dramatically enhance elasticity even for very stiff nanocomposite materials made by layer-by-layer (LBL) assembly.[17,26−29] This approach made preparation of deformable plasma electrodes from high-strength conductive nanocomposites possible—something that was previously considered to be technologically challenging.[17] The versatile chemistry and uniformity of LBL and some other nanocomposites afford effective patterning and etching modes that open the door to the deterministic design of patterns to obtain complex, specific optical effects upon mechanical deformation.

DOI: 10.1021/acsnano.6b02096
ACS Nano 2016, 10, 6156–6162

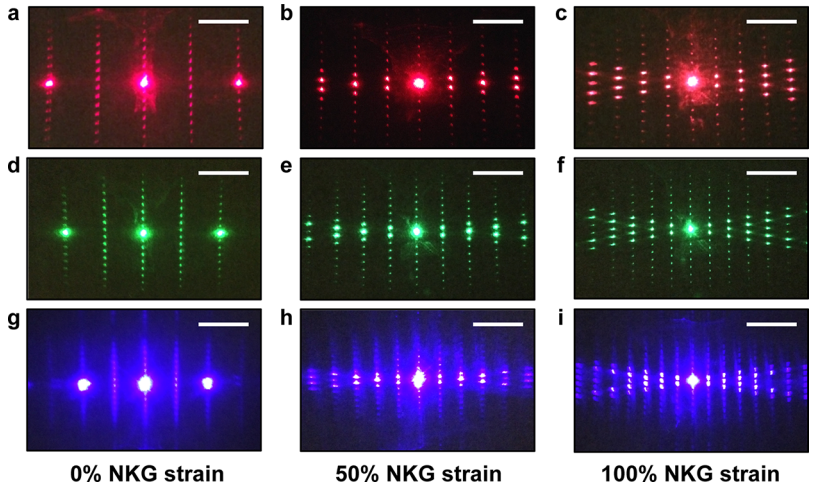

Figure 2. Laser diffraction patterns in transmission mode generated by NKGs based on Cr/Parylene C nanocomposites. (a−g) Diffraction patterns generated using 635 nm (a−c), 532 nm (d−f), and 450 nm (g−i) laser beams under 0% (a,d,g), 50% (b,e,h), and 100% (c,f,i) NKG strains. Scale bars: 25 mm.

Therefore, we decided to look into the possibilities of utilizing kirigami composites with microscale and nanoscale features for tunable optical gratings to address their materials challenges. Here, we show that kirigami sheets from stiff/strong nanocomposites can serve as tunable diffraction gratings. They perform similarly or better than surface-grooved elastomers and produce intense sophisticated diffraction patterns even in the case of a simple parallel notch pattern. Unlike MEMS diffraction devices, nanocomposite kirigami gratings (NKGs) allow for device engineering in the visible spectral range. The large deformations that kirigami materials can enable wide-angle beam steering and open the path for a family of reconfigurable optical elements.

RESULTS AND DISCUSSION

We explore two examples of typical nanocomposite materials. The first material platform is based on a 1.5 μm poly(*p*-xylylene) (Parylene C) substrate coated with a nanoscale layer of chromium with a thickness of ∼40 nm (Figure S1) deposited on a layer of PMMA with a thickness of 100 nm. This latter component of this trilayer stack is sacrificial and is subsequently dissolved to release the patterned film from the substrate. The chromium film reduces optical transmission in the areas where no notches are made, which is desirable for diffraction, while its nanoscale thickness affords greater elasticity than, for instance, solid chromium foil. In the framework of this study, it is significant that Parylene C is a relatively stiff material with a Young's modulus of ∼4.5 GPa and a yield strength of ∼60 MPa.[30] Despite its advantageous mechanical properties, environmental robustness, and simplicity of fabrication and etching, it was not used as a tunable surface-grooved diffraction grating because Parylene C has a low elastic limit of ∼0.015.[30]

In another materials platform, the nanoscale chromium thin film is substituted with a layer of a carbon nanotube/poly(vinyl alcohol) (CNT/PVA) composite (∼100 nm in thickness) prepared by 30 cycles of LBL assembly (Figures S1 and S2).[31,32] The CNT/PVA composites offer similar optical opaqueness but with a significantly higher limit of stretching deformation with failure strains as high as 0.2,[31,32] compared with typical failure strains of metallic thin films in the range of 0.002 to 0.05.[33−35] A large variety of LBL nanocomposites can be made from nanoscale "building blocks" with a diverse range of optical properties.[36−38] Given the nanoscale uniformity and controllability of LBL nanocomposites,[38−40] this technique has capabilities to greatly diversify the diffraction optics.

To manufacture NKGs, the layered stacks of both types of nanocomposites were lithographically patterned with 1.5 μm × 60 μm slits (Figure 1a−d and Figure S3). Here, we chose kirigami patterns based on the combination of the following factors: (1) macroscopic stretchability of the kirigami device and (2) effectiveness as diffraction grating. Kirigami based on parallel slits represents a simple case with these two requirements being satisfied. The thin film is then released from the substrate (Figure 1c) by selective dissolution or etching of certain material components (PMMA or SiO_2). The free-standing NKGs can be reversibly stretched to afford dynamic manipulation of light propagation (Figure 1d). Note that the nanocomposite coating in the NKG devices serves as the active optical element, while Parylene C serves as the structural support for the devices. This stiff plastic material is simple to integrate with a variety of actuators and a wide range of nanocomposite coatings. One can anticipate that reconfigurable NKG elements made solely from the LBL nanocomposite can be made. Such a configuration will be advantageous by the better mechanics of the material, environmental resilience, and lower mass compared with NKGs on a plastic support. However, it will also require engineering approaches for actuation, which are the subject of the ongoing study.

Their ability to diffract light can be demonstrated by an optical image of NKGs supported on a glass wafer (Figure 1e). Scanning electron microscopy (SEM) (Quanta 200, FEI) reveals the microscale morphology of NKGs. Figure 1f,g shows the microstructures of NKGs under 0 and 100% strains in the lateral direction (*i.e.*, the direction perpendicular to the microscale slits), respectively; the values of NKG strains are defined by the fractional increase of total length of the patterned structures, compared to the original relaxed state. The variability of periodicity and 3D orientation of NKG surface features under different deformation states indicate their potential capabilities as tunable diffraction gratings.

Lasers with various wavelengths (*i.e.*, λ = 635, 532, and 450 nm) were used to generate transmissive diffraction patterns from NKGs under various levels of strain (Figure 2). The clear

DOI: 10.1021/acsnano.6b02096
ACS Nano 2016, 10, 6156−6162

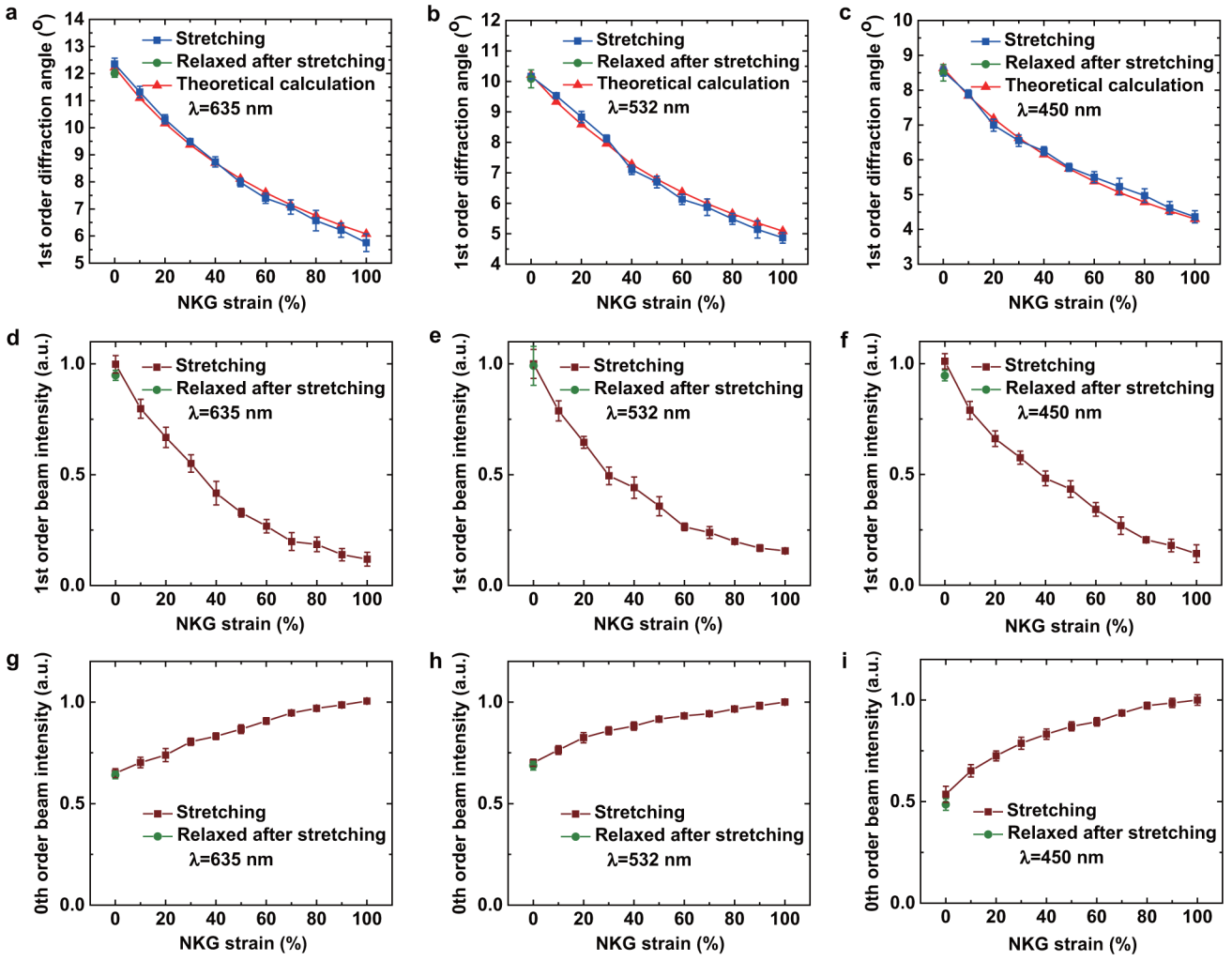

Figure 3. Experimental and theoretical light diffraction patterns for NKGs. (a–c) Experimental data and theoretical calculations of the first-order diffraction angle obtained for (CNT/PVA)/ Parylene C nanocomposite gratings as a function of the NKG strain for 635 nm (a), 532 nm (b), and 450 nm (c) laser beams. (d–f) Normalized intensity of the first-order diffracted beam as a function of the NKG strain for 635 nm (d), 532 nm (e), and 450 nm (f) laser beams. (g–i) Normalized intensity of the zeroth-order beam as a function of the NKG strain for 635 nm (g), 532 nm (h), and 450 nm (i) laser beams. Error bars denote standard deviation.

patterns generated by lasers beams (refer to the Materials and Methods section) indicate that the NKGs can maintain periodic slit sequence over macroscopic length scale even under 100% NKG strain. The lateral spacing in diffraction patterns shows distinct correlation with the NKG strain, which is consistent with the reciprocal relationship between the dimensions in the diffraction pattern and the spacing of the corresponding grating known from classical optics (Figure 3). As expected, the longitudinal spacing in the diffraction patterns exhibits a dependency on the NKG strain weaker than that of the lateral one, due to the relatively small changes in longitudinal periodicity with lateral direction of the deformation. The diffraction patterns also show significant dependence on the wavelength of the incident laser beam.

NKGs are elastic and spontaneously recover to the relaxed geometry when the stress is removed. They enable cyclic mechanical actuation that can also be loosely referred to as 4D kirigami (Video S1) that includes three dimensions of the kirigami composite patterns plus one time dimension characteristic for oscillatory reconfiguration. The diffracted beams form patterns determined by the uniaxial strain of the NKG that represents dynamic, wavelength-dependent beam steering.

Quantitative analyses of obtained diffraction patterns are instructive when evaluating the performance of NKGs. The optical characteristics of the first-order beam diffracted in the lateral direction (Figures S3 and S4) were considered in this study as the key indicator of diffraction grating performance. The experimental data for the first-order diffraction angles as a function of the NKG strain (Figure 3a–c) are compared to theoretical predictions obtained from a variant of the classical grating equation:

$$d(1 + \varepsilon)\sin\theta_m = m\lambda \quad (1)$$

where d is the spacing of the slits without stretch (3 μm in this work), ε is the applied NKG strain, θ_m is the mth-order diffraction angle, and λ is the wavelength of the incident laser. The experimental results of the first-order diffraction angle show excellent agreement with theoretical predictions (Figure 3a–c). The angular dynamic range for the diffracted beams with $m = 1$, as defined by the ratio between the maximum value obtained from the original relaxed state and the minimum value obtained with 100% NKG strain, is nearly 2:1 for all of the tested wavelengths. The angular range for steering of the first-order beam reaches as large as 6.5° for a 635 nm laser beam. In

DOI: 10.1021/acsnano.6b02096
ACS Nano 2016, 10, 6156–6162

Table 1. Quantitative Comparison of NKG with Other Reported Tunable Grating Techniques

techniques	ref	tunability of grating period (% of minimum period)	minimum grating period (μm)	angular range for beam steering of visible light (degree)	operation modes
NKG	present work	100	3	6.5 (635 nm laser)	transmissive/ reflective
surface-grooved elastomer	8−10	22−32	0.8−1		reflective
	12	100	0.8		
	11	18	4.5	1 (633 nm laser)	transmissive
MEMS	13	125	720		reflective
	14	0.2	4	0.02 (633 nm laser)	

addition to the diffraction angle, the intensities of the first-order and zeroth-order beams also show significant correlation with the strain (Figure 3d−i), which is likely to be related to the change in slit geometry when laterally deformed (Figure 1f,g). The experimental data for NKGs based on (CNT/PVA)/Parylene C (Figure 3) and Cr/Parylene C (Figures S5−S7) agree with each other, which indicates the predictability of diffraction behavior. The measurements also quantitatively confirm the stability of the NKGs under cyclic actuation, where 100 deformation cycles do not degrade the device performance (Figures S8−S11). Extended exposure to ambient indoor light for ~3 months and laser illumination for ~6 h did not affect their appearance or performance.

Side-by-side quantitative comparison of NKG performance as diffraction gratings with respect to previously reported tunable gratings is given in Table 1. As one can see, NKGs generate some of the highest order diffraction patterns while extending the dynamic range of the grating period for beam steering. Moreover, NKGs also allow for both transmissive and reflective operation modes, which is essential for on-chip integration for semiconductor optoelectronics.[5,41,42]

Microscale mechanics can give insight into the reason for the high performance of NKGs as diffraction optical elements and their mechanical robustness. Finite element methods (FEM) were used to investigate the strain distribution of NKGs under lateral deformation (Figure 4a−c). SEM images of the corresponding units are also presented for comparison (Figure 4d−f). As we observed in Figure 2 by optical means, stretching

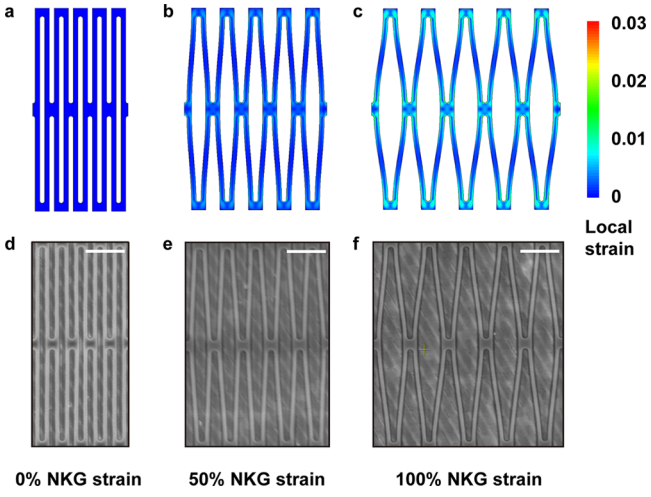

Figure 4. Strain distribution in NKGs. (a−c) FEM simulation of an element of NKG sheet under 0% (a), 50% (b), and 100% (c) NKG strain. (d−f) SEM images of the corresponding NKGs based on Cr/Parylene C nanocomposites under 0% (d), 50% (e), and 100% (f) NKG strain. Scale bars: 10 μm.

of NKGs results in the lateral expansion of the kirigami sheets, with a minimal effect on the longitudinal spacing in stark contrast to, for instance PDMS and other elastomer-based diffraction gratings. Due to the presence of a pattern of the microscale slits, the macroscopic strain is distributed uniformly among individual microscale periodic units, with the large deformation accommodated by bending of the kirigami "flaps" formed between the nearest slits. Importantly, the strain of NKG as a whole is uniformly distributed in the nanocomposite sheet between the numerous local deformation points, avoiding stochastic concentration on a few selected defects.[17] Thus, even under 100% NKG strain, the local strain level remains far below the failure strain of the structural material and is mostly within the elastic deformation regime (<0.015).[30] Hence, it becomes possible to make diffraction gratings and realize their reversible reconfiguration even from very stiff materials.

CONCLUSIONS

Kirigami patterns were previously utilized as a source of concepts for deformable structural units of electronic components,[15] solar cells,[43] and flexible/stretchable electronics[16,44] as well as for addressing the materials challenges of plasma electrodes.[17] Here, we demonstrated that microscale kirigami materials can also be used in diffraction optics to produce variable-period gratings from nanocomposites. While further tests using different reconfigurability modes are still needed, the prepared prototypes of beam steering optical elements raise the hope that the materials challenge of strain-tunable gratings can be addressed using kirigami nanocomposites. The expansive library of high-performance nanomaterials previously unavailable for diffraction gratings is expected to improve device robustness and widen the gratings' angular range. The three-dimensional character of kirigami surfaces offers high efficiency and additional opportunities for modulation of light polarization. The simplicity of their time-dependent reconfiguration, *i.e.* the fourth dimension, offers beam steering capabilities. Kirigami composites made with different geometrical designs and from a large library of composite materials can provide a versatile route for engineering of diffraction optics components, including subwavelength devices. Their utility as optical modulators and optoelectronic systems in the visible, short-wave IR, near-IR, far-IR, and terahertz wavelength ranges should also be further explored.

MATERIALS AND METHODS

NKG Fabrication. *Cr/Parylene C Nanocomposites:* Solution-based poly(methyl methacrylate) (PMMA 950, MicroChem) is spin-coated (3000 rpm) on a 4 in. glass wafer and baked subsequently on a 180 °C hot plate to remove the solvent. Parylene C (SCS Inc.) is deposited on the PMMA-coated glass wafer by a commercially available vacuum deposition system (PDS 2035CR, SCS Inc.), forming a thin film with ~1.5 μm thickness. A thin film of chromium (~40

DOI: 10.1021/acsnano.6b02096
ACS Nano 2016, 10, 6156−6162

nm) is then deposited on top of the Parylene C by sputtering (Lab 18, Kurt J. Lesker). Photolithography processes (GCA AS200 Autostep) generate a patterned photoresist (S1813, Shipley) on top of the thin film composites. The corresponding patterns in the thin film composites are then formed by wet etching of Cr followed by reactive ion etching (Plasmatherm 790) of Parylene C. After these steps, the wafer is soaked in acetone for 8 h to dissolve the PMMA layer and to release the patterned thin film composites from the glass substrate, leading to free-standing NKGs.

(CNT/PVA)/Parylene C Composites: The CNT/PVA nanocomposite layer is deposited on a 4 in. glass wafer. The detailed processing for CNT/PVA nanocomposites appears elsewhere.[31] Briefly, alternating dipping processes for the glass substrate into an aqueous dispersion of poly(styrenesulfonate)-stabilized carbon nanotubes (0.5 mg/mL) and 0.2 wt % poly(vinyl alcohol) (MW ~ 13 000−23 000, Sigma-Aldrich) aqueous solution, with rinsing and drying processes between the dipping steps, generate a uniform nanocomposite thin film. Thirty repeated cycles of CNT and PVA dipping steps form a thin film with a thickness of ~100 nm. A Parylene C layer (~1.5 μm in thickness) is then deposited on the CNT/PVA composites, followed by depositing a Cr thin film (~40 nm) on Parylene C. The patterning processes for the composites here are identical to the steps for PMMA/Parylene C/Cr; however, the Cr layer here only serves as the mask for the reactive ion etching. After the patterning, the Cr layer is removed by wet etching, and the wafer is soaked in hydrofluoric acid (0.1 wt %) for 8 h to release the NKGs from the glass substrate.

NKG Characterization. Free-standing NKGs are transferred onto another transparent glass wafer, with a small amount of water applied between for lubricating during actuation. The measurements are performed with a custom setup (Figure S4). Lasers with 635 nm wavelength and ~1.5 mm beam diameter (Beam of Light Technologies), 532 nm wavelength with ~1 mm beam diameter (Logitech), and 450 nm wavelength with ~3 mm beam diameter (Beam of Light Technologies) are illuminated individually from the direction normal to the plane of NKGs. Two pieces of silicone elastomer are brought into uniform contact with the ends of the NKGs for applying a stretch during the experiments. The lasers are diffracted from three different locations on the NKGs in each stretching state for the statistics. Diffraction angles are determined by measuring the corresponding distance in the diffraction pattern as well as the distance between the grating and the screen. Light intensity of the diffracted beam is characterized using a commercial photometer (54-018, Edmund Optics).

FEM Simulations. Commercial software (ANSYS 14.0) is employed to simulate the deformation and strain distribution of NKGs. A model consisting of five unit cells of the NKG structure is constructed in the software, with the thickness of the thin film t = 1.5 μm, the Young's modulus of the material E = 4.5 GPa, and the Poisson's ratio of the material ν = 0.4. Static structural analysis accompanied by SOLID 185 element is applied, with an approximate global mesh size of 0.15 μm. Boundary conditions are enforced on both left and right ends of the model. The left boundary is fixed with no displacement allowed in any direction. A uniaxial tensile load is applied on the right boundary of the model with the displacement constrained in the tensile direction. There is no geometrical constraint applied on the rest of the model. H-Method processed with the SPARSE solver is applied for simulating the finite element model.

ASSOCIATED CONTENT

Supporting Information

The Supporting Information is available free of charge on the ACS Publications website at DOI: 10.1021/acsnano.6b02096.

Figures S1−S13 (PDF)

Video S1, a NKG under cyclic actuation with diffraction patterns generated with a 532 nm laser (AVI)

AUTHOR INFORMATION

Corresponding Author

*E-mail: kotov@umich.edu.

Notes

The authors declare no competing financial interest.

ACKNOWLEDGMENTS

The central part of this work was supported by NSF projects 1403777, 1411014, 1463474, and 1538180. This work was performed in part at the University of Michigan Lurie Nanofabrication Facility and Electron Microbeam Analysis Laboratory. The authors thank Ms. Xi Liao for the help with illustrations.

REFERENCES

(1) Sun, J.; Timurdogan, E.; Yaacobi, A.; Hosseini, E. S.; Watts, M. R. Large-scale nanophotonic phased array. *Nature* **2013**, *493*, 195−199.
(2) Aksyuk, V. A.; Pardo, F.; Carr, D.; Greywall, D.; Chan, H. B.; Simon, M. E.; Gasparyan, A.; Shea, H.; Lifton, V.; Bolle, C.; Arney, S.; Frahm, R.; Paczkowski, M.; Haueis, M.; Ryf, R.; Neilson, D. T.; Kim, J.; Giles, C. R.; Bishop, D. Beam-Steering Micromirrors for Large Optical Cross-Connects. *J. Lightwave Technol.* **2003**, *21*, 634−642.
(3) Fischer, B.; Sternklar, S. Self Bragg Matched Beam Steering Using the Double Color Pumped Photorefractive Oscillator. *Appl. Phys. Lett.* **1987**, *51*, 74.
(4) Masuda, S.; Takahashi, S.; Nose, T.; Sato, S.; Ito, H. Liquid-Crystal Microlens with a Beam-Steering Function. *Appl. Opt.* **1997**, *36*, 4772.
(5) Kurosaka, Y.; Iwahashi, S.; Liang, Y.; Sakai, K.; Miyai, E.; Kunishi, W.; Ohnishi, D.; Noda, S. On-Chip Beam-Steering Photonic-Crystal Lasers. *Nat. Photonics* **2010**, *4*, 447−450.
(6) Rinne, S. A.; García-Santamaría, F.; Braun, P. V. Embedded Cavities and Waveguides in Three-Dimensional Silicon Photonic Crystals. *Nat. Photonics* **2008**, *2*, 52−56.
(7) Tuantranont, A.; Bright, V. M.; Zhang, J.; Zhang, W.; Neff, J. A.; Lee, Y. C. Optical Beam Steering Using MEMS-Controllable Microlens Array. *Sens. Actuators, A* **2001**, *91*, 363−372.
(8) Ghisleri, C.; Siano, M.; Ravagnan, L.; Potenza, M. A. C.; Milani, P. Nanocomposite-Based Stretchable Optics. *Laser Photon. Rev.* **2013**, *7*, 1020−1026.
(9) Yu, C.; O'Brien, K.; Zhang, Y.-H.; Yu, H.; Jiang, H. Tunable Optical Gratings Based on Buckled Nanoscale Thin Films on Transparent Elastomeric Substrates. *Appl. Phys. Lett.* **2010**, *96*, 041111.
(10) Aschwanden, M.; Stemmer, A. Polymeric, Electrically Tunable Diffraction Grating Based on Artificial Muscles. *Opt. Lett.* **2006**, *31*, 2610.
(11) Simonov, A. N.; Akhzar-Mehr, O.; Vdovin, G. Light Scanner Based on a Viscoelastic Stretchable Grating. *Opt. Lett.* **2005**, *30*, 949−951.
(12) Ghisleri, C.; Potenza, M. A. C.; Ravagnan, L.; Bellacicca, A.; Milani, P. A Simple Scanning Spectrometer Based on a Stretchable Elastomeric Reflective Grating. *Appl. Phys. Lett.* **2014**, *104*, 061910.
(13) Monnai, Y.; Altmann, K.; Jansen, C.; Hillmer, H.; Koch, M.; Shinoda, H. Terahertz Beam Steering and Variable Focusing Using Programmable Diffraction Gratings. *Opt. Express* **2013**, *21*, 2347−2354.
(14) Wong, C. W.; Jeon, Y.; Barbastathis, G.; Kim, S.-G. Analog Tunable Gratings Driven by Thin-Film Piezoelectric Microelectromechanical Actuators. *Appl. Opt.* **2003**, *42*, 621−626.
(15) Song, Z.; Wang, X.; Lv, C.; An, Y.; Liang, M.; Ma, T.; He, D.; Zheng, Y.-J.; Huang, S.-Q.; Yu, H.; Jiang, H. Kirigami-Based Stretchable Lithium-Ion Batteries. *Sci. Rep.* **2015**, *5*, 10988.
(16) Zhang, Y.; Yan, Z.; Nan, K.; Xiao, D.; Liu, Y.; Luan, H.; Fu, H.; Wang, X.; Yang, Q.; Wang, J.; Ren, R.; Si, H.; Liu, F.; Yang, L.; Li, H.; Wang, J.; Guo, X.; Luo, H.; Wang, L.; Huang, Y.; Rogers, J. A. A Mechanically Driven Form of Kirigami as a Route to 3D

DOI: 10.1021/acsnano.6b02096
ACS Nano 2016, 10, 6156−6162

Mesostructures in Micro/nanomembranes. *Proc. Natl. Acad. Sci. U. S. A.* **2015**, *112*, 11757.
(17) Shyu, T. C.; Damasceno, P. F.; Dodd, P. M.; Lamoureux, A.; Xu, L.; Shlian, M.; Shtein, M.; Glotzer, S. C.; Kotov, N. A. A Kirigami Approach to Engineering Elasticity in Nanocomposites through Patterned Defects. *Nat. Mater.* **2015**, *14*, 785−789.
(18) Blees, M. K.; Barnard, A. W.; Rose, P. A.; Roberts, S. P.; McGill, K. L.; Huang, P. Y.; Ruyack, A. R.; Kevek, J. W.; Kobrin, B.; Muller, D. A.; McEuen, P. L. Graphene Kirigami. *Nature* **2015**, *524*, 204.
(19) Cho, Y.; Shin, J.-H.; Costa, A.; Kim, T. A.; Kunin, V.; Li, J.; Lee, S. Y.; Yang, S.; Han, H. N.; Choi, I.-S.; Srolovitz, D. J. Engineering the Shape and Structure of Materials by Fractal Cut. *Proc. Natl. Acad. Sci. U. S. A.* **2014**, *111*, 17390−17395.
(20) Gracias, D. H.; Kavthekar, V.; Love, J. C.; Paul, K. E.; Whitesides, G. M. Fabrication of Micrometer-Scale, Patterned Polyhedra by Self-Assembly. *Adv. Mater.* **2002**, *14*, 235−238.
(21) Saito, K.; Agnese, F.; Scarpa, F. A Cellular Kirigami Morphing Wingbox Concept. *J. Intell. Mater. Syst. Struct.* **2011**, *22*, 935−944.
(22) Hawkes, E.; An, B.; Benbernou, N. M.; Tanaka, H.; Kim, S.; Demaine, E. D.; Rus, D.; Wood, R. J. Programmable Matter by Folding. *Proc. Natl. Acad. Sci. U. S. A.* **2010**, *107*, 12441−12445.
(23) Overvelde, J. T. B.; Shan, S.; Bertoldi, K. Compaction through Buckling in 2D Periodic, Soft and Porous Structures: Effect of Pore Shape. *Adv. Mater.* **2012**, *24*, 2337−2342.
(24) Zhang, Y.; Matsumoto, E. A.; Peter, A.; Lin, P. C.; Kamien, R. D.; Yang, S. One-Step Nanoscale Assembly of Complex Structures *via* Harnessing of an Elastic Instability. *Nano Lett.* **2008**, *8*, 1192−1196.
(25) Qi, Z.; Campbell, D. K.; Park, H. S. Atomistic Simulations of Tension-Induced Large Deformation and Stretchability in Graphene Kirigami. *Phys. Rev. B: Condens. Matter Mater. Phys.* **2014**, *90*, 245437.
(26) Jiang, C.; Markutsya, S.; Pikus, Y.; Tsukruk, V. V. Freely Suspended Nanocomposite Membranes as Highly Sensitive Sensors. *Nat. Mater.* **2004**, *3*, 721−728.
(27) Tang, Z.; Kotov, N. A.; Magonov, S.; Ozturk, B. Nanostructured Artificial Nacre. *Nat. Mater.* **2003**, *2*, 413−418.
(28) Mamedov, A. A.; Kotov, N. a; Prato, M.; Guldi, D. M.; Wicksted, J. P.; Hirsch, A. Molecular Design of Strong Single-Wall Carbon Nanotube/polyelectrolyte Multilayer Composites. *Nat. Mater.* **2002**, *1*, 190−194.
(29) Podsiadlo, P.; Kaushik, A. K.; Arruda, E. M.; Waas, A. M.; Shim, B. S.; Xu, J.; Nandivada, H.; Pumplin, B. G.; Lahann, J.; Ramamoorthy, A.; Kotov, N. A. Ultrastrong and Stiff Layered Polymer Nanocomposites. *Science* **2007**, *318*, 80−83.
(30) Shih, C. Y.; Harder, T. A.; Tai, Y. C. Yield Strength of Thin-Film Parylene-C. *Microsyst. Technol.* **2004**, *10*, 407−411.
(31) Shim, B. S.; Tang, Z.; Morabito, M. P.; Agarwal, A.; Hong, H.; Kotov, N. A. Integration of Conductivity, Transparency, and Mechanical Strength into Highly Homogeneous Layer-by-Layer Composites of Single-Walled Carbon Nanotubes for Optoelectronics. *Chem. Mater.* **2007**, *19*, 5467−5474.
(32) Shim, B. S.; Zhu, J.; Jan, E.; Critchley, K.; Kotov, N. A. Transparent Conductors from Layer-by-Layer Assembled SWNT Films: Importance of Mechanical Properties and a New Figure of Merit. *ACS Nano* **2010**, *4*, 3725−3734.
(33) Cordill, M. J.; Taylor, A.; Schalko, J.; Dehm, G. Fracture and Delamination of Chromium Thin Films on Polymer Substrates. *Metall. Mater. Trans. A* **2010**, *41*, 870−875.
(34) Lee, H. J.; Zhang, P.; Bravman, J. C. Tensile Failure by Grain Thinning in Micromachined Aluminum Thin Films. *J. Appl. Phys.* **2003**, *93*, 1443−1451.
(35) Huang, H.; Spaepen, F. Tensile Testing of Free-Standing Cu, Ag and Al Thin Films and Ag/Cu Multilayers. *Acta Mater.* **2000**, *48*, 3261−3269.
(36) Kim, Y.; Yeom, B.; Arteaga, O.; Yoo, S. J.; Lee, S.-G.; Kim, J.-G.; Kotov, N. A. Reconfigurable Chiroptical Nanocomposites with Chirality Transfer from the Macro- to the Nanoscale. *Nat. Mater.* **2016**, *15*, 461−468.
(37) Jiang, C.; McConney, M. E.; Singamaneni, S.; Merrick, E.; Chen, Y.; Zhao, J.; Zhang, L.; Tsukruk, V. V. Thermo-Optical Arrays of Flexible Nanoscale Nanomembranes Freely Suspended over Microfabricated Cavities as IR Microimagers. *Chem. Mater.* **2006**, *18*, 2632−2634.
(38) Hiller, J.; Mendelsohn, J. D.; Rubner, M. F. Reversibly Erasable Nanoporous Anti-Reflection Coatings from Polyelectrolyte Multilayers. *Nat. Mater.* **2002**, *1*, 59−63.
(39) Decher, G.; Schlenoff, J. B. *Multilayer Thin Films: Sequential Assembly of Nanocomposite Materials*, 2nd ed.; Wiley-VCH: Weinheim, Germany, 2012.
(40) Jiang, C.; Tsukruk, V. V. Freestanding Nanostructures *via* Layer-by-Layer Assembly. *Adv. Mater.* **2006**, *18*, 829−840.
(41) Fattal, D.; Peng, Z.; Tran, T.; Vo, S.; Fiorentino, M.; Brug, J.; Beausoleil, R. G. A Multi-Directional Backlight for a Wide-Angle, Glasses-Free Three-Dimensional Display. *Nature* **2013**, *495*, 348−351.
(42) Huang, M. C. Y.; Zhou, Y.; Chang-Hasnain, C. J. A Surface-Emitting Laser Incorporating a High-Index-Contrast Subwavelength Grating. *Nat. Photonics* **2007**, *1*, 297−297.
(43) Lamoureux, A.; Lee, K.; Shlian, M.; Forrest, S. R.; Shtein, M. Dynamic Kirigami Structures for Integrated Solar Tracking. *Nat. Commun.* **2015**, *6*, 8092.
(44) Ahn, B. Y.; Shoji, D.; Hansen, C. J.; Hong, E.; Dunand, D. C.; Lewis, J. A. Printed Origami Structures. *Adv. Mater.* **2010**, *22*, 2251−2254.

DOI: 10.1021/acsnano.6b02096
ACS Nano 2016, 10, 6156−6162